Published May 26, 2008

The VEGF receptor Flt-1 spatially modulates Flk-1 signaling and blood vessel branching

Nicholas C. Kappas,[1] Gefei Zeng,[1] John C. Chappell,[1] Joseph B. Kearney,[2] Surovi Hazarika,[4] Kimberly G. Kallianos,[1] Cam Patterson,[3] Brian H. Annex,[4] and Victoria L. Bautch[1,2,3]

[1]Department of Biology, [2]Program in Genetics and Molecular Biology, and [3]Carolina Cardiovascular Biology Center, The University of North Carolina at Chapel Hill, Chapel Hill, NC 27599
[4]Division of Cardiology, Duke University, Durham, NC 27710

Blood vessel formation requires the integrated regulation of endothelial cell proliferation and branching morphogenesis, but how this coordinated regulation is achieved is not well understood. Flt-1 (vascular endothelial growth factor [VEGF] receptor 1) is a high affinity VEGF-A receptor whose loss leads to vessel overgrowth and dysmorphogenesis. We examined the ability of Flt-1 isoform transgenes to rescue the vascular development of embryonic stem cell–derived *flt-1*$^{-/-}$ mutant vessels. Endothelial proliferation was equivalently rescued by both soluble (sFlt-1) and membrane-tethered (mFlt-1) isoforms, but only sFlt-1 rescued vessel branching. Flk-1 Tyr-1173 phosphorylation was increased in *flt-1*$^{-/-}$ mutant vessels and partially rescued by the Flt-1 isoform transgenes. sFlt-1–rescued vessels exhibited more heterogeneous levels of pFlk than did mFlt-1–rescued vessels, and reporter gene expression from the *flt-1* locus was also heterogeneous in developing vessels. Our data support a model whereby sFlt-1 protein is more efficient than mFlt-1 at amplifying initial expression differences, and these amplified differences set up local discontinuities in VEGF-A ligand availability that are important for proper vessel branching.

Introduction

Angiogenesis is of critical importance to blood vessel formation in developing embryos and in physiological and pathological conditions (for reviews see Risau, 1997; Coultas et al., 2005). During angiogenesis, endothelial cells respond to both proliferative signals and morphogenetic cues to extend simple vascular structures and form and expand a branching plexus. Although several signaling pathways important in angiogenesis have been identified, relatively little is known about how these signals are regulated to coordinate vessel branching and endothelial cell proliferation.

The VEGF-A signaling pathway is a crucial mediator of endothelial cell division and migration during angiogenesis (for reviews see Kowanetz and Ferrara, 2006; Shibuya and Claesson-Welsh, 2006). The VEGF-A pathway requires tight dose-dependent regulation for proper blood vessel formation because minor changes in the amount of VEGF-A adversely affect vascular development, and the loss of even one copy of the *vegfa* gene leads to embryonic lethality (Carmeliet et al., 1996; Ferrara et al., 1996; Bautch et al., 2000; Miquerol et al., 2000). VEGF-A signaling is modulated by alternative splicing of VEGF-A RNA to produce three major isoforms (Tischer et al., 1991). These VEGF-A isoforms have differing affinities for heparin that are predicted to lead to differential distribution from VEGF-A–producing cells, and genetic manipulation of these isoforms leads to vessel dysmorphogenesis (Ruhrberg et al., 2002; Stalmans et al., 2002). Recent studies by Gerhardt et al. (2003) support a model in which the spatial context of VEGF-A ligand presentation to the endothelial cell is important for vessel morphogenesis, whereas endothelial cell proliferation is regulated by the local VEGF-A concentration in a spatially independent manner.

The biological effects of VEGF-A are mediated by two high affinity receptor tyrosine kinases expressed on endothelial cells: flk-1 (VEGFR-2) and flt-1 (VEGFR-1). VEGF-A signaling through flk-1 positively regulates endothelial cell division and migration, whereas the function of flt-1 is less clear (for reviews see Rahimi, 2006; Shibuya, 2006). Deletion of

N.C. Kappas and G. Zeng contributed equally to this paper.

Correspondence to Victoria L. Bautch: bautch@med.unc.edu

N.C. Kappas's present address is Synapse Medical Communications, New York, NY 10017.

Abbreviations used in this paper: ES, embryonic stem; PECAM, platelet endothelial cell adhesion molecule; WT, wild type.

The online version of this article contains supplemental material.

Supplemental Material can be found at:
http://jcb.rupress.org/content/suppl/2008/05/26/jcb.200709114.DC1.html

The Rockefeller University Press $30.00
J. Cell Biol. Vol. 181 No. 5 847–858
www.jcb.org/cgi/doi/10.1083/jcb.200709114

Published May 26, 2008

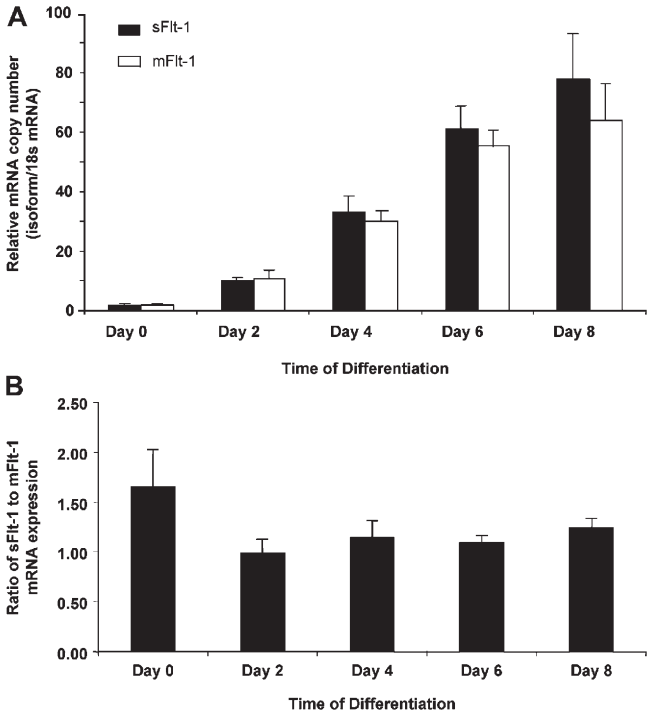

Figure 1. **Flt-1 isoform expression during a developmental time course.** WT ES cell cultures were used (day 0) or differentiated for the indicated number of days, and total RNA was isolated for real-time PCR analysis. (A) The relative copy number of sFlt-1 or mFlt-1 RNAs were calculated relative to 18S RNA. (B) The ratio of sFlt-1/mFlt-1 RNA over time. Error bars represent SEM.

flt-1 in mice results in embryonic lethality at midgestation with vascular defects, and deletion of *flt-1* in mouse embryonic stem (ES) cell–derived vessels leads to the overproliferation of endothelial cells and dysmorphogenesis of vessels (Fong et al., 1995; Kearney et al., 2002, 2004). Flt-1 mRNA is alternatively spliced to encode both a full-length receptor tyrosine kinase (mFlt-1) and a soluble isoform (sFlt-1) that contains the VEGF-A–binding extracellular domain (Kendall and Thomas, 1993). VEGF-A has a higher affinity for Flt-1 than for Flk-1, so both Flt-1 isoforms can potentially sequester VEGF-A and modulate signaling through Flk-1. *Flt-1*$^{-/-}$ ES cell–derived vessels have approximately threefold higher levels of activated Flk-1 than do normal vessels as measured by overall levels of tyrosine phosphorylation, which is consistent with a role for Flt-1 in ligand sequestration during development (Roberts et al., 2004). Moreover, mice lacking the cytoplasmic tail of the Flt-1 receptor are viable, indicating that the signaling function of Flt-1 is not essential during embryonic development (Hiratsuka et al., 1998). Collectively, these data suggest that Flt-1 functions in vascular development as a ligand sink to bind and sequester VEGF-A, and in this way Flt-1 regulates signaling through the Flk-1 receptor. However, how the two Flt-1 isoforms contribute to this regulation has not been elucidated.

We hypothesized that the Flt-1 isoforms have differential effects on endothelial proliferation and branching morphogenesis in developing vessels. To test this hypothesis, we reintroduced isoform-specific Flt-1 transgenes into *flt-1*$^{-/-}$ vessels. We found soluble Flt-1 to be highly effective at rescuing branching morphogenesis relative to membrane-bound Flt-1, whereas both membrane-tethered and soluble Flt-1 rescued endothelial cell proliferation equivalently. Moreover, expression from the *flt-1* locus was heterogeneous in developing vessels, and the level of Flk-1 phosphorylation on individual endothelial cells in developing vessels was more heterogeneous in sFlt-1–rescued vessels than in mFlt-1–rescued vessels, suggesting that sFlt-regulated spatial discontinuities in Flk-1 signaling derived from heterogeneous *flt-1* locus expression are required for proper branching morphogenesis. Our results support a model in which VEGF-A ligand presentation is modulated by Flt-1 isoform production in the target endothelial cells to ensure proper vessel morphogenesis.

Results

Both flt-1 isoforms are expressed in developing blood vessels

To determine the relative expression levels of Flt-1 (VEGFR-1) isoforms during vascular development, we used real-time PCR with isoform-specific primers for sFlt-1 or mFlt-1 (Fig. 1; Hazarika et al., 2007). This analysis showed that, as expected, the expression levels of both isoforms were increased over the time course of development of ES cell–derived vessels (Fig. 1 A). Moreover, comparison showed that the relative proportions of each isoform were roughly equivalent and that the relative proportions did not significantly change during the time course of differentiation (Fig. 1 B). These data indicate that both sFlt-1 and mFlt-1 are expressed during vascular development and provide a rationale for investigating the effects of each isoform on vascular development.

Transgenes encoding individual Flt-1 isoforms targeted into the ROSA26 locus rescue the *flt-1*$^{-/-}$ vessel phenotype

ES cell–derived vessels lacking both Flt-1 isoforms have an increased endothelial cell mitotic index (Kearney et al., 2002) and a morphogenetic defect that results in reduced sprouting and branch formation (Kearney et al., 2004). To directly assess the role of the soluble (sFlt-1) and membrane-bound (mFlt-1) Flt-1 isoforms on endothelial cell division and vessel morphogenesis, we targeted sFlt-1 and mFlt-1 isoform transgenes linked to the platelet endothelial cell adhesion molecule (PECAM) promoter/enhancer into the *ROSA26* genomic locus of *flt-1*$^{-/-}$ ES cells (Fig. 2). Transgenes targeted to the *ROSA26* locus of ES cells are present as a single copy rather than long concatamers, and they have uniform expression levels (Soriano, 1999; Srinivas et al., 2001). This strategy allowed for the direct comparison of rescue properties of the sFlt-1 and mFlt-1 isoform transgenes. The transgenes were linked to the PECAM promoter/enhancer because this regulatory region results in the expression of transgenes in developing blood vessels (Kearney et al., 2004). After electroporation of the targeting constructs, drug-resistant *flt-1*$^{-/-}$ ES colonies were selected, and correct targeting by homologous recombination was confirmed by PCR (unpublished data).

Published May 26, 2008

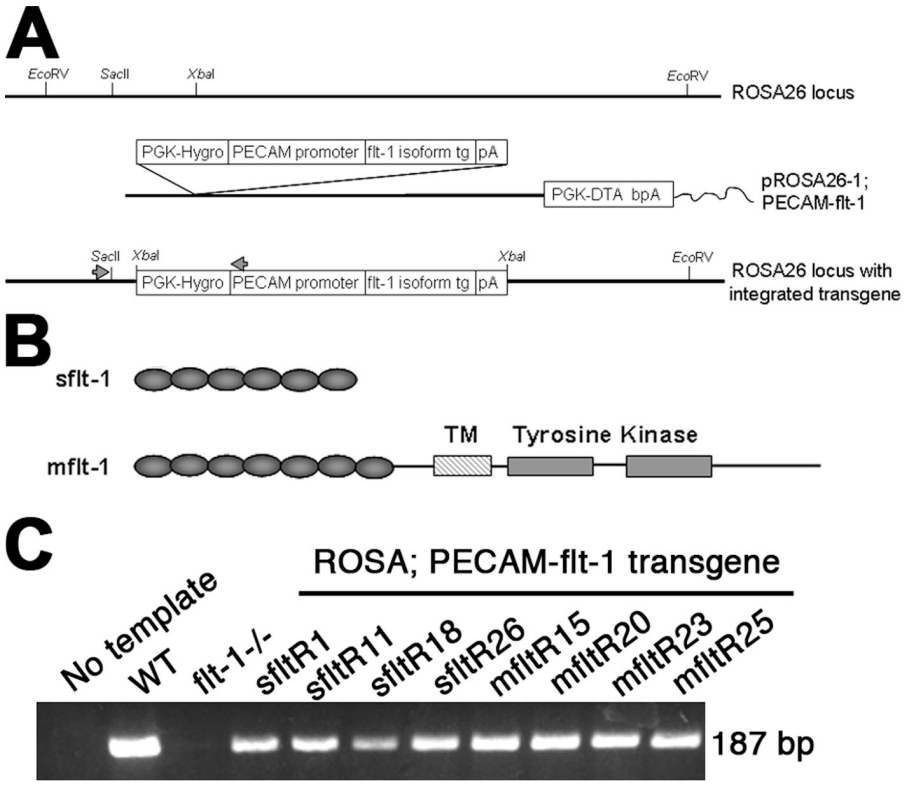

Figure 2. ***ROSA26* locus–targeted Flt-1 isoform rescue clones.** (A) Flt-1 isoform transgene *ROSA26* targeting. (top) Restriction map of the *ROSA26* locus. (middle) pROSA26-1–containing insertion cassette of PECAM promoter/enhancer, Flt-1 isoform, and a hygromycin B selectable marker with PGK–diptheria toxin A cassette for negative selection. (bottom) Predicted structure of the *ROSA26* locus after integration of the pROSA26-1 insertion cassette in *flt-1*$^{-/-}$ ES cells. Arrows denote primers used to verify correct targeting into *flt-1*$^{-/-}$ ES cells (not depicted). (B) Diagram of individual Flt-1 isoforms. Soluble Flt-1 (sFlt-1) and membrane-localized Flt-1 (mFlt-1) each contain an extracellular VEGF-A–binding domain consisting of Ig domains (gray circles). Only mFlt-1 contains a transmembrane domain region (TM) and a tyrosine kinase domain. (C) Total RNA was isolated from differentiated day 8 wild-type (WT), *flt-1*$^{-/-}$, *flt-1*$^{-/-;Tg\ ROSA\text{-}PECAM\text{-}sflt\text{-}1}$, and *flt-1*$^{-/-;Tg\ ROSA\text{-}PECAM\text{-}mflt\text{-}1}$ cultures and analyzed by semi-quantitative RT-PCR using *flt-1* primers.

From a group of 10–15 rescue clones with each isoform, we selected four clones each of the ROSA26sFlt-1 and ROSA26mFlt-1 genotype for further analysis. These *flt-1*$^{-/-;Tg\ PECAM\text{-}flt\text{-}1ROSA}$ ES cell clones were differentiated to day 8, and the expression of individual Flt-1 isoform transgenes was verified by RT-PCR, showing little heterogeneity in expression levels from the *ROSA26* locus (Fig. 2 C). The differentiated cultures were also labeled with PECAM antibody to visualize developing blood vessels (Fig. 3). Compared with *flt-1*$^{-/-}$ cultures, all Flt-1 isoform transgene clones showed a partial rescue of vascular development (Fig. 3, compare A and B with C–J). The rescue clones had fewer areas of overt vessel dysmorphogenesis and endothelial sheets and more areas of branching. Thus, targeting of PECAM promoter/enhancer-driven Flt-1 isoform transgenes to the ROSA26 genomic locus leads to rescue of the *flt-1*$^{-/-}$ mutant vessel phenotype.

Isoform-specific differences in rescue phenotypes of Flt-1 transgenes

Close visual inspection of the Flt-1 isoform transgene rescue clones suggested isoform-specific differences in the rescue phenotypes (Fig. 3). Specifically, although the rescue of vessel area appeared similar in all clones, the group of sFlt-1 isoform rescue clones had a rescue of branching morphogenesis that was not seen in the mFlt-1 isoform rescue clones (Fig. 3, compare C–F with G–J). To quantify the Flt-1 isoform rescue phenotypes, PECAM-stained cultures were analyzed for the percentage of vessel area, as measured by the PECAM-positive area relative to the total cellular area of the culture (Fig. 4 A). We previously showed that this parameter reflects the endothelial mitotic index and is thus a measure of endothelial cell proliferation (Kearney et al., 2002). Compared with controls (wild-type [WT] mean = 16.5%; *flt-1*$^{-/-}$ mean = 53.4%), all rescue clones partially rescued vessel area (sFlt rescue mean = 24.2%; mFlt rescue mean = 24.1%), and no consistent differences were seen between the groups of sFlt-1 and mFlt-1 rescue clones (Fig. 4 A). In contrast, analysis of vessel morphogenesis by branch point analysis showed that compared with controls (WT mean = 12.6 branches/millimeter; *flt-1*$^{-/-}$ mean = 7.8 branches/millimeter), sFlt-1 rescue clones significantly rescued branching (sFlt rescue mean = 9.8 branches/millimeter), whereas the group of mFlt-1 rescue clones did not significantly rescue branching (mFlt rescue mean = 8.2 branches/millimeter; Fig. 4 B). Thus, the *ROSA26* locus–targeted clones exhibited differential rescue effects on the *flt-1*$^{-/-}$ mutant vessels; vessel area was equivalently rescued by both Flt-1 isoforms, whereas vessel morphogenesis was only rescued by the sFlt-1 isoform.

To further verify that the changes in vessel area reflected the rescue of endothelial proliferation, we analyzed a subset of each group of Flt-1 isoform rescue clones for two additional parameters. We performed FACS analysis for an independent endothelial marker, ICAM-2, and found a similar pattern in that all analyzed Flt-1 rescue clones had endothelial cell numbers that were intermediate between Flt-1 mutant vessels and WT vessels (Fig. S1, available at http://www.jcb.org/cgi/content/full/jcb.200709114/DC1). Next, we calculated the endothelial mitotic index for the same subset of rescue clones and found that all Flt-1 isoform rescue clones had endothelial mitotic indices at or near that of WT vessels and significantly different from that of *flt-1*$^{-/-}$ mutant vessels (Fig. 5). Thus, all Flt-1 isoform rescue clones had a partial rescue of vessel area, the number of endothelial cells, and the endothelial mitotic index relative to *flt-1*$^{-/-}$

Published May 26, 2008

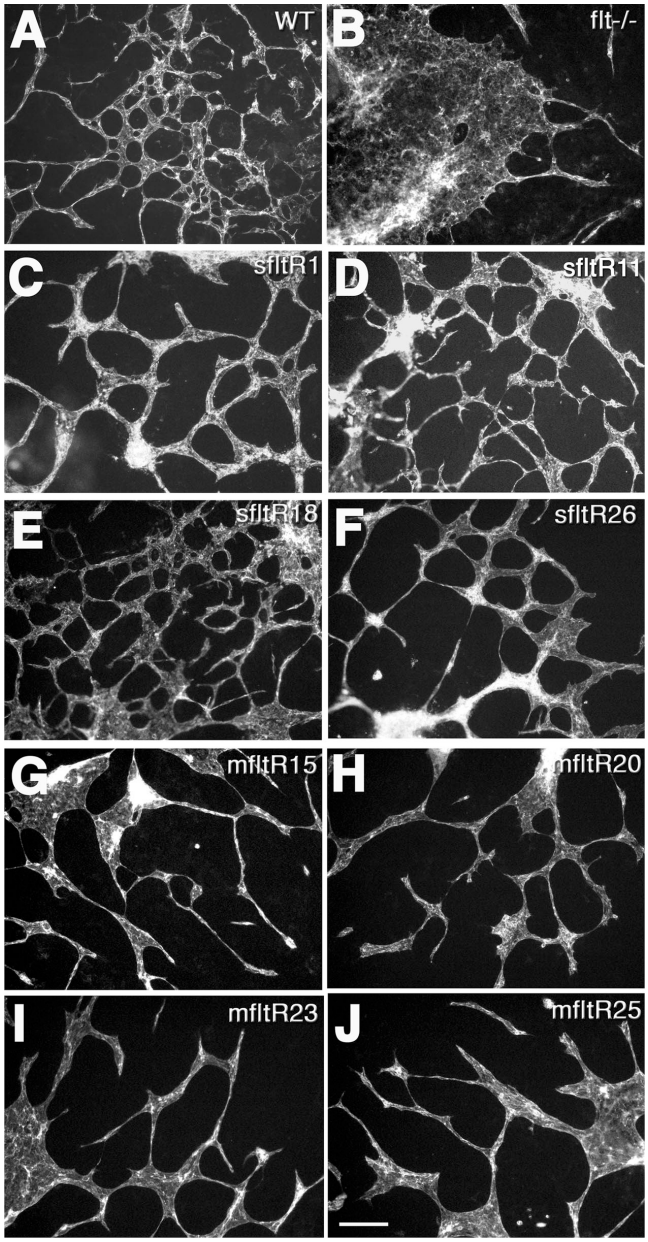

Figure 3. ***ROSA26*-targeted Flt-1 isoforms rescue *flt-1*$^{-/-}$ mutant vessel dysmorphogenesis.** Day 8 differentiated ES cultures were stained for PECAM. All transgenic clones partially rescued the vessel dysmorphogenesis of *flt-1*$^{-/-}$ vessels (B). Note that targeted sFlt-1 transgene *ROSA26* clones (C–F) appear to have more branched vessels than do targeted mFlt-1 transgene *ROSA26* clones (G–J). Clone numbers are indicated in the top right of each frame. Bar, 200 µm.

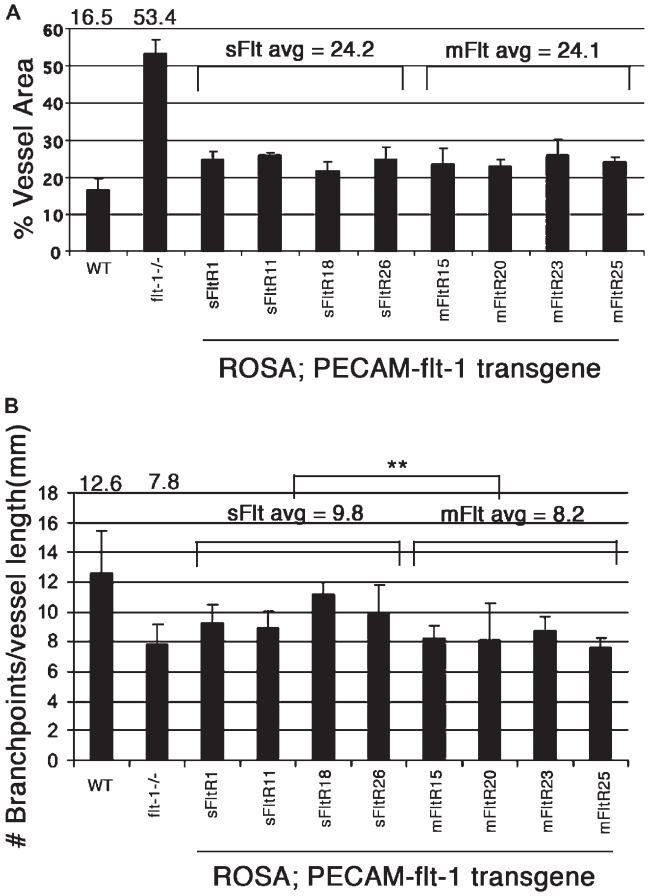

Figure 4. ***ROSA26*-targeted Flt-1 isoforms differentially rescue *flt-1*$^{-/-}$ mutant vessel parameters.** (A and B) Day 8 differentiated ES cell cultures were reacted with the PECAM antibody, and representative areas were analyzed for vessel area (A) or branch point frequency (B). (A) The mean vessel area of all rescue clones was significantly different from WT and *flt-1*$^{-/-}$ mutant clones (*flt-1*$^{-/-}$ vs. sFlt and mFlt, $P \leq 0.0005$; WT vs. sFlt and mFlt, $P \leq 0.02$) but did not differ between sFlt-1 and mFlt-1 rescue clones (sFlt vs. mFlt, $P = 0.86$). (B) The mean branch points/millimeter vessel length was significantly different between sFlt-1 and mFlt-1 rescue clones (sFlt vs. mFlt, **, $P \leq 0.03$). Branch points/millimeter vessel length was not significantly different between *flt-1*$^{-/-}$ mutant and mFlt clones (*flt-1*$^{-/-}$ vs. mFlt, $P = 0.97$; WT vs. mFlt, $P \leq 0.01$). Branch points/millimeter vessel length was significantly different between *flt-1*$^{-/-}$ mutant and sFlt isoform clones (*flt-1*$^{-/-}$ vs. sFlt, $P \leq 0.01$; WT vs. sFlt, $P = 0.16$). Error bars represent SEM.

mutant cultures, showing that all *ROSA26* locus–targeted rescue clones partially rescue endothelial cell proliferation.

Flt-1 isoform transgenes modulate signaling through the Flk-1 receptor

Tyrosine phosphorylation of the Flk-1 receptor is increased in the absence of Flt-1, consistent with a model in which Flt-1 normally negatively modulates signaling through Flk-1 (Roberts et al., 2004). To determine how the Flt-1 isoforms affected signaling through Flk-1, we assayed specific phosphorylation at Flk-1 Tyr-1173 (equivalent to Tyr-1175 in VEGFR-2; Fig. 6) because this tyrosine is essential for blood vessel formation and embryonic viability (Sakurai et al., 2005). Analysis of the level of Flk-1 Tyr-1173 phosphorylation (pFlk) relative to total Flk-1 by Western blotting showed the expected increase in the ratio for the Flt-1 mutant culture, and the ROSA locus–targeted Flt-1 isoform rescue clones had ratios largely intermediate between mutant and WT cultures (Fig. 6, A and B).

Differentiated ES cell cultures were double stained for total Flk-1 and pFlk and examined by confocal microscopy (Fig. 7). The Flk-1–positive cells were scored as being positive or negative for pFlk (Fig. 7, A and B). Consistent with the results of the Western blot, the confocal analysis showed that a higher proportion of Flk-1–expressing cells were positive for pFlk in *flt-1*$^{-/-}$ mutant vessels (30%) compared with WT vessels (17%), and the *ROSA26* locus–targeted Flt-1 isoform

Published May 26, 2008

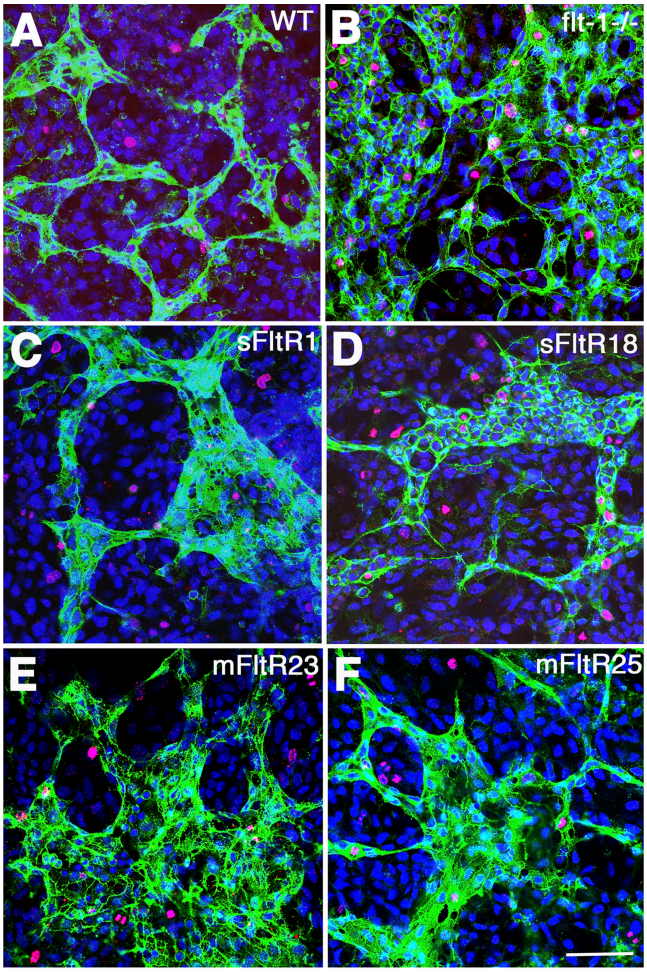

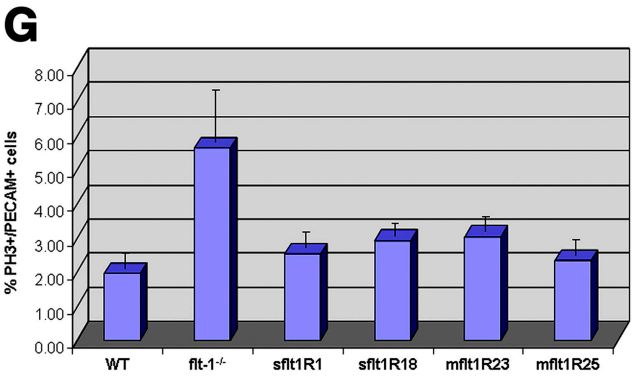

Figure 5. ***ROSA26*-targeted Flt-1 isoform transgenes partially rescue the endothelial cell mitotic index.** (A–F) Day 7 differentiated cultures were fixed and stained for PECAM-1 (green), the mitotic marker antiphosphohistone H3 (red), and the nuclear dye DRAQ 5 (blue). (G) Representative confocal images were scored by counting the PECAM-positive nuclei and the percentage that reacted with the phosphohistone antibody to calculate the endothelial mitotic index. Error bars represent SEM. χ^2 analysis showed that the WT endothelial mitotic index was significantly different from *flt-1*$^{-/-}$ mutants (χ^2 = 15.1; P ≤ 0.0001), and each of the Flt-1 isoform rescue clones differed from *flt-1*$^{-/-}$ mutants (sFltR1: χ^2 = 12.2; P ≤ 0.0005; sFltR18: χ^2 =7.6; P ≤ 0.005; mFltR23: χ^2 = 7.5; P ≤ 0.008; mFltR25: χ^2 = 13.0; P ≤ 0.0003). Bar, 50 µm.

rescue clones had values that were largely intermediate between the two controls (Fig. 7 B). Neither analysis showed consistent differences between the sFlt-1–rescued vessels and the mFlt-1–rescued vessels.

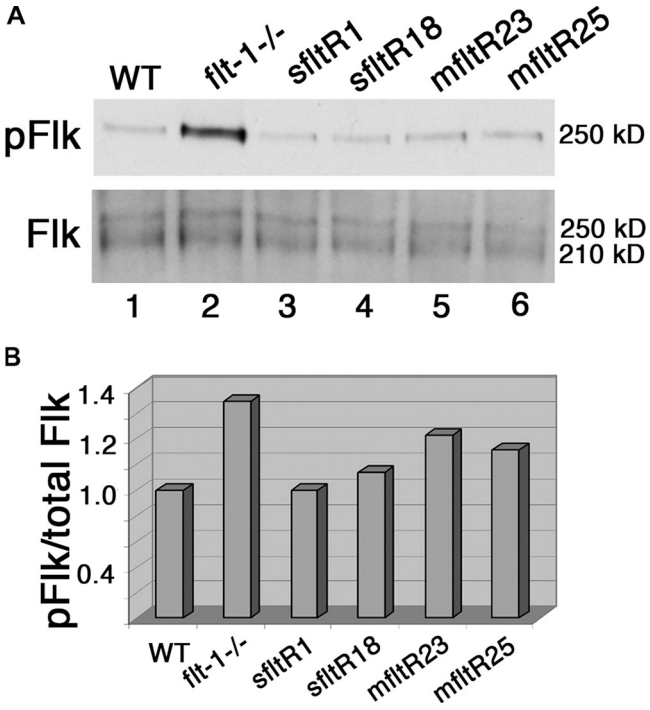

Figure 6. ***ROSA26*-targeted Flt-1 isoform transgenes partially rescue the ratio of pFlk to total Flk-1.** Day 8 differentiated cultures were processed for Western blot analysis with antibodies to total Flk-1 and pFlk (Tyr-1173/1175). (A, top) The signal from hybridization with pFlk antibody. (bottom) Hybridization with a total Flk-1 antibody. All rescue clones tested partially rescued the increased pFlk signal seen in the *flt-1*$^{-/-}$ mutant cultures (compare lane 2 with lanes 3–6). (B) Quantitation of the normalized signals from a representative experiment.

However, visual examination of the pFlk/total Flk double-stained vessels in the different *flt-1* genetic backgrounds suggested that the pFlk staining patterns differed (Fig. 7 A). In a given vessel that was Flk-1 positive, WT vessels showed a mosaic pattern of pFlk staining, with some cells showing a relatively strong pFlk signal relative to other cells in the same vessel (Fig. 7 A, a–d). In contrast, *flt-1*$^{-/-}$ mutant vessels had more uniform pFlk-1 staining along a given Flk-1–positive vessel (Fig. 7 A, e–h). The *ROSA26* locus–targeted sFlt-1–rescued vessels showed a similar mosaic pattern of pFlk staining as seen in the WT vessels, whereas the mFlt-1–rescued vessels resembled the *flt-1*$^{-/-}$ mutant vessels in having a more homogeneous pattern of pFlk staining (Fig. 7 A, i–p). To quantify these results, double-stained pFlk/total Flk-positive endothelial cells in vessels were analyzed using imaging software to determine individual ratios of pFlk to total Flk signal (Fig. 7 C). The distribution of ratios was very similar in WT and sFlt-1–rescued vessels. For example, only 8.0% (2/25) of WT and 8.3% (2/24) of sFltR18 endothelial cells had pFlk/total Flk ratios between 0.2 and 0.3. In contrast, *flt-1*$^{-/-}$ mutant vessels and mFlt-1–rescued vessels had a different distribution of ratios. In these genetic backgrounds, 48% (12/25) of *flt-1*$^{-/-}$ mutant and 33% (7/21) of mFltR23 endothelial cells had pFlk/total Flk ratios between 0.2 and 0.3. These findings suggest that the mosaic distribution of Flk-1 signaling in endothelial cells is important for proper vascular morphogenesis and that the sFlt-1 isoform but not the mFlt-1 isoform rescues this aspect of VEGF signaling.

Published May 26, 2008

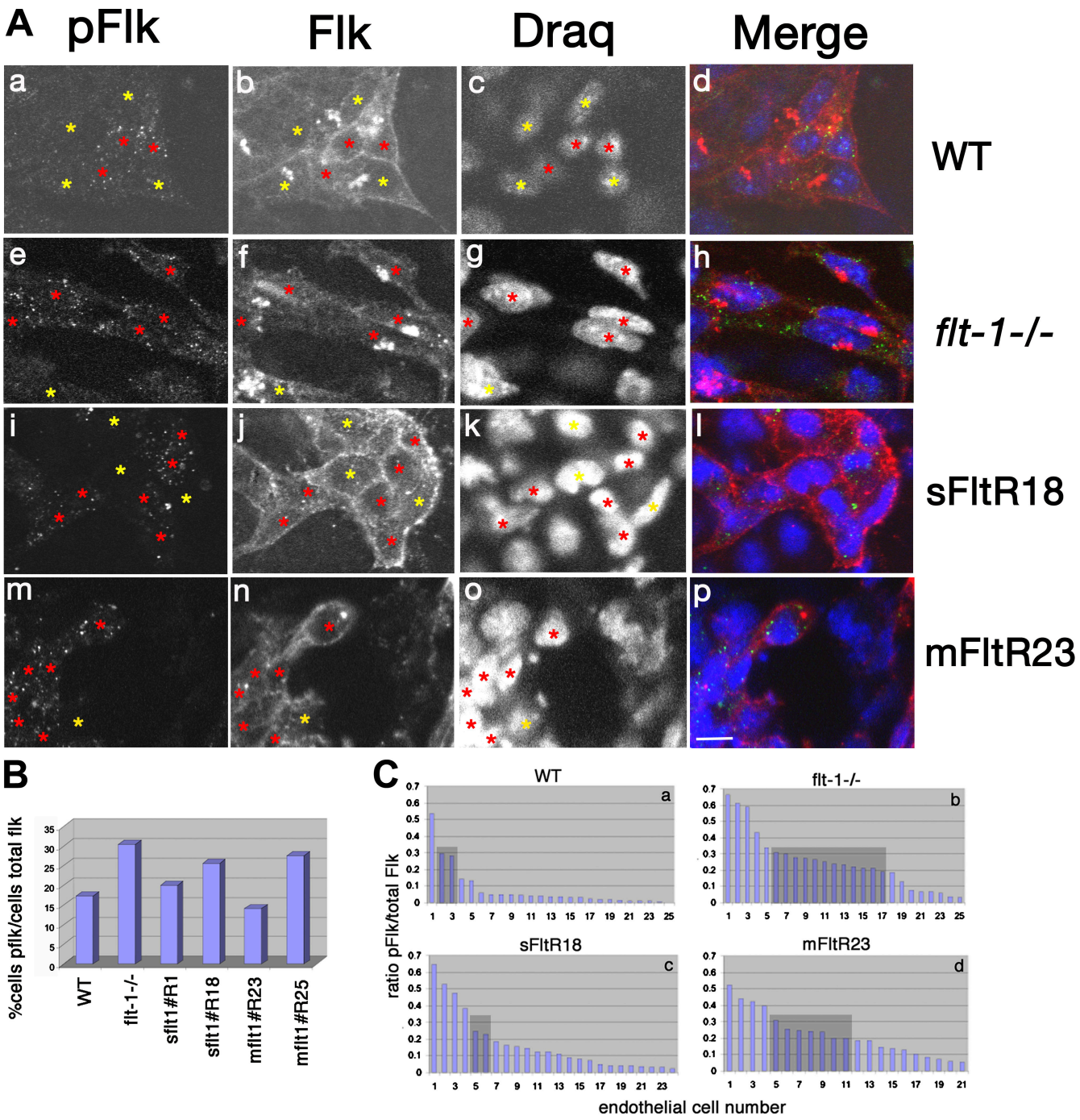

Figure 7. ***ROSA26*-targeted sFlt-1 isoform transgene preferentially rescues the mosaic endothelial expression of pFlk (Tyr-1173).** Day 8 differentiated cultures were fixed and stained with antibodies to total Flk-1 and pFlk (Tyr-1173/1175). (A) ES-derived vessels were visualized by staining for pFlk in green (a, e, I, and m), total Flk in red (b, f, j, and n), and DRAQ 5 in blue to visualize nuclei (c, g, k, and o). In a–c, e–g, i–k, and m-o, red asterisks denote endothelial cells with moderate to high levels of pFlk, and yellow asterisks denote endothelial cells with none to low levels of pFlk. Note that pFlk-positive endothelial cells are mosaic in WT (a–d), and *flt-1*$^{-/-}$ endothelial cells have more uniform high levels of pFlk (e–h). Expression of the sFlt-1 transgene (i–l) recreates the heterogeneous pattern of pFlk vessel staining, whereas expression of the mFlt-1 transgene (m–p) does not lead to heterogeneity of staining. (B) Stained cultures were visualized for total Flk, and the same cells were scored as positive or negative for pFlk. Percentages of a representative experiment are shown on the y axis. (C) Individual endothelial cells were outlined and analyzed for the ratio of pFlk/total Flk using imaging software. The numbers were graphed in order of descending ratios for each genotype. In each graph, the darker areas show the number of cells that had pFlk/total Flk ratios between 0.2 and 0.3. Bar, 10 µm.

To begin to determine how sFlt-1 expression leads to heterogeneity of the pFlk signal, we examined reporter gene expression from the *flt-1* locus in developing vessels using readout of the *lacZ* gene inserted into the *flt-1* locus in *flt-1*$^{+/-}$ and *flt-1*$^{-/-}$ ES cell–derived vessels (Fig. 8). The levels of β-galactosidase reporter expression varied quite dramatically in areas of *flt-1*$^{-/-}$ vessels, with some cells having strong staining relative to nearby cells with little to no staining (Fig. 8, A–H). To verify that expression differences also existed in a nonmutant background, we examined phenotypically normal *flt-1*$^{+/-}$ vessels and found evidence of heterogeneity in

Published May 26, 2008

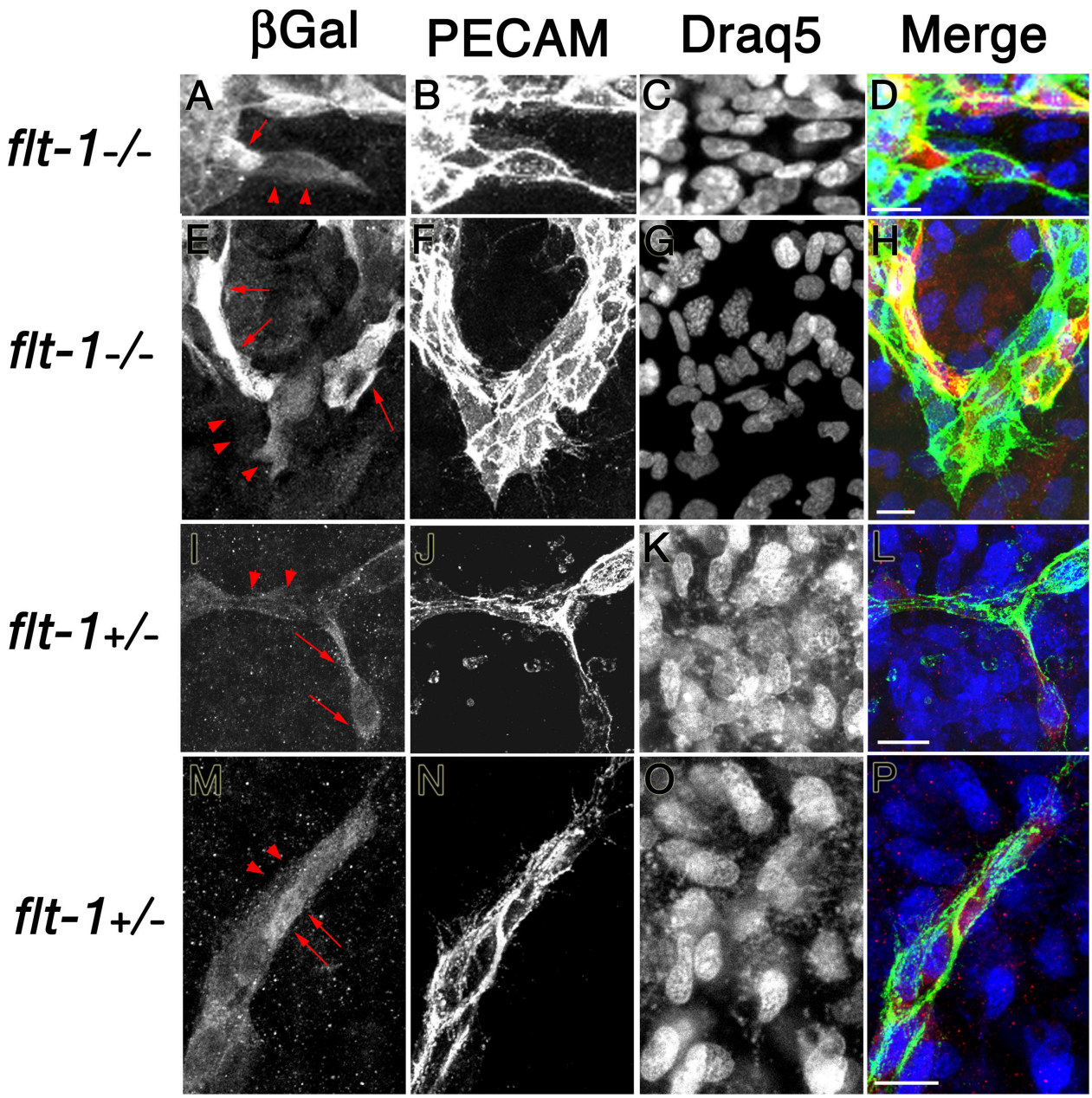

Figure 8. **Expression of β-galactosidase from the *flt-1* locus reveals heterogenous endothelial cell expression in developing vessels.** Day 8 differentiated cultures were fixed and stained with antibodies to β-galactosidase and PECAM-1. (A–H) *flt-1*$^{-/-}$ mutant vessels. (I–P) *flt-1*$^{+/-}$ heterozygous (phenotypically normal) vessels. ES-derived vessels were visualized by staining for β-galactosidase in red (A, E, I, and M), PECAM-1 in green (B, F, J, and N), and DRAQ 5 in blue to visualize nuclei (C, G, K, and O). In A, E, I, and M, red arrows denote endothelial cells with moderate to high levels of β-galactosidase, and red arrowheads denote endothelial cells with none to low levels of β-galactosidase. All panels are z-stack compilations of 12-μm thickness to avoid sampling heterogeneity, with the exception of K and O, which are single confocal images from the stack. Bars, 10 μm.

reporter gene expression levels among nearby endothelial cells in developing vessels (Fig. 8, I–P). These findings suggest that Flt-1 RNA is expressed heterogeneously from the *flt-1* locus and that initial differences in *flt-1* locus expression are differentially amplified by sFlt-1 protein over mFlt-1 protein, leading to the observed heterogeneity of pFlk staining seen in the sFlt-1–rescued vessels.

Discussion

Our results show that two Flt-1 isoforms produced by endothelial cells have differential effects on developing vessels. Both the soluble and membrane-localized Flt-1 isoform transgenes rescue endothelial proliferation to equivalent levels, but they affect branching morphogenesis in different ways. The soluble Flt-1 isoform transgene but not the membrane-tethered Flt-1 isoform transgene rescues vessel branching morphogenesis, and the different branching rescue phenotypes correlate with different patterns of Flk-1 activation in developing vessels. These findings suggest that the ability of sFlt-1 to bind and sequester VEGF-A at a distance from the endothelial cell surface is important for proper vessel morphogenesis, and, thus, endothelial cells of developing vessels provide critical input for their own morphogenesis.

Published May 26, 2008

Previously, the *flt-1* genomic locus was modified in vivo to a locus that generated both sFlt-1 and mFlt-1 without the cytoplasmic domain (Hiratsuka et al., 1998). This nonsignaling locus was compatible with embryonic vascular development, which is consistent with our data, but the role of individual Flt-1 isoforms was not tested. Recently, the *flt-1* locus was modified in vivo to a locus that generated only the sFlt-1 isoform (Hiratsuka et al., 2005). The resulting embryos were viable on certain genetic backgrounds and partially viable on others, suggesting that sFlt-1 is sufficient to promote proper vascular development in vivo in the appropriate genetic background. It is compelling that both genetic manipulation of the endogenous *flt-1* locus and rescue via transgene expression of the different Flt-1 isoforms yield evidence that sFlt-1 has a critical role in vascular development. Our data provide the first direct comparison of the ability of the different Flt-1 isoforms to rescue specific aspects of vascular development, and we show here that vessel branching is uniquely sensitive to the soluble isoform of the Flt-1 receptor.

Targeting of each Flt-1 isoform transgene independently to the *ROSA26* locus also allowed us to separate the effects of sFlt-1 and mFlt-1 on specific parameters of vessel development. Our analysis revealed that sFlt-1–expressing clones were able to rescue vessel branching to significant levels, whereas the mFlt-1 clones did not rescue vessel branching. In contrast, both Flt-1 isoform transgenes rescued vessel area, endothelial cell numbers, and the endothelial mitotic index to equivalent levels. These findings suggest that differences between the two Flt-1 isoforms are not relevant to the ability of Flt-1 to rescue endothelial proliferation, but they are critical to the role of sFlt-1 in vessel branching morphogenesis. The major differences between the Flt-1 isoforms are that the soluble isoform cannot signal, but it can diffuse away from the endothelial cell and into the matrix (Orecchia et al., 2003), whereas the membrane-tethered isoform cannot diffuse but can theoretically signal. However, our preliminary data show that mFlt-1 deleted for the cytoplasmic signaling domain has the same rescue profile as intact mFlt-1 (unpublished data), as expected from the finding that deleted mFlt-1 can support embryonic vascular development (Hiratsuka et al., 1998). Thus, the differences in the ability to rescue vascular development between the two Flt-1 isoforms reside primarily in the putative spatial location of the different isoforms. Flt-1 can form heterodimers with Flk-1, although these interactions have been difficult to analyze with receptors at endogenous levels (Autiero et al., 2003; Neagoe et al., 2005). However, if heterodimer formation is relevant during vascular development, the mFlt-1 isoform would presumably have an advantage in forming heterodimers over sFlt-1 because it is membrane localized near Flk-1; therefore, this mechanism is unlikely to account for the increased efficiency of sFlt-1 in the rescue of vessel branching morphogenesis developmentally. Thus, the most likely model is that during vascular development, both Flt-1 isoforms act as ligand sinks to sequester VEGF-A, and this property is sufficient to regulate the amplitude of the VEGF signal and rescue endothelial proliferation independent of spatial context. However, the unique ability of sFlt-1 to leave the cell surface provides additional spatial regulation of VEGF signaling and rescues branching morphogenesis.

How does the soluble form of the Flt-1 receptor impact vessel morphogenesis? The three major VEGF-A isoforms are hypothesized to have different spatial distributions in the extracellular matrix that are important in regulating vessel morphogenesis, perhaps by formation of a gradient. In support of this model, mice expressing either only VEGF-A_{120}, which lacks a heparin-binding domain, or VEGF-A_{188}, with multiple heparin-binding domains, have retinas with perturbed migration of vascular tip cell filopodia and aberrant vessel morphogenesis (Ruhrberg et al., 2002; Gerhardt et al., 2003). sFlt-1 contains a heparin-binding domain (Park and Lee, 1999), and it also binds the extracellular matrix upon release from the endothelial cell in addition to binding and sequestering the VEGF-A ligand (Orecchia et al., 2003). Thus, secreted Flt-1 may spread uniformly from the endothelial cell and, in a quantitative fashion, regulate the presentation of VEGF-A that is already established. In other developmental contexts, cells respond differentially to gradients of the same morphogen in specific concentration ranges, so the interaction between VEGF-A and sFlt-1, even if quantitative, could change the morphogenetic response of the endothelial cell to VEGF-A (for review see Ashe and Briscoe, 2006). Alternatively, sFlt-1 might establish a countergradient or some other configuration that modulates VEGF-A presentation to endothelial cells qualitatively as well. We favor the latter model because it is consistent with the differences in *flt-1* locus expression and distribution of Flk-1 activation that we documented in developing vessels (Fig. 9). In either scenario, the ability of sFlt-1 to move away from the endothelial cell after secretion is critical to its mechanism of action.

Filopodia form and extend from growing vascular cells into the extracellular matrix. Filopodia are involved in sensing the environment in other systems, such as guidance of the neuronal growth cone (for review see Koleske, 2003). Analysis of retinal vessels indicates that endothelial tip cells differ from neighboring endothelial stalk cells in the number of filopodia and expression of marker genes, implicating filopodia as transducers of positional information (Gerhardt et al., 2003). Our data support and extend this model by revealing a required role for sFlt-1 in providing positional information. We found that Flk-1 activation, as measured by the phosphorylation of Tyr-1173, is not normally uniform in developing vessels, but it exhibits a mosaic pattern. In many cases, small groups of endothelial cells had higher levels of pFlk staining than neighboring endothelial cells, suggesting that these cells experience higher levels of Flk-1 activation. In contrast, *flt-1*$^{-/-}$ mutant vessels had both higher levels and a more homogeneous distribution of pFlk staining, suggesting that spatial information required for different levels of Flk-1 activation in different endothelial cells is missing in the *flt-1*$^{-/-}$ mutant genetic background. This implies that Flt-1 provides that spatial information, at least in part. We found that a *lacZ* reporter gene inserted into the *flt-1* locus is expressed at different levels among endothelial cells of developing vessels. This finding strongly suggests that endogenous Flt-1 RNA is also expressed heterogeneously in developing vessels, and it provides a starting point for a model of how heterogeneity of Flt-1 expression may lead to a mosaic pFlk signal (Fig. 9). However, the ability of sFlt-1 but not mFlt-1 to rescue branching morphogenesis and the

Published May 26, 2008

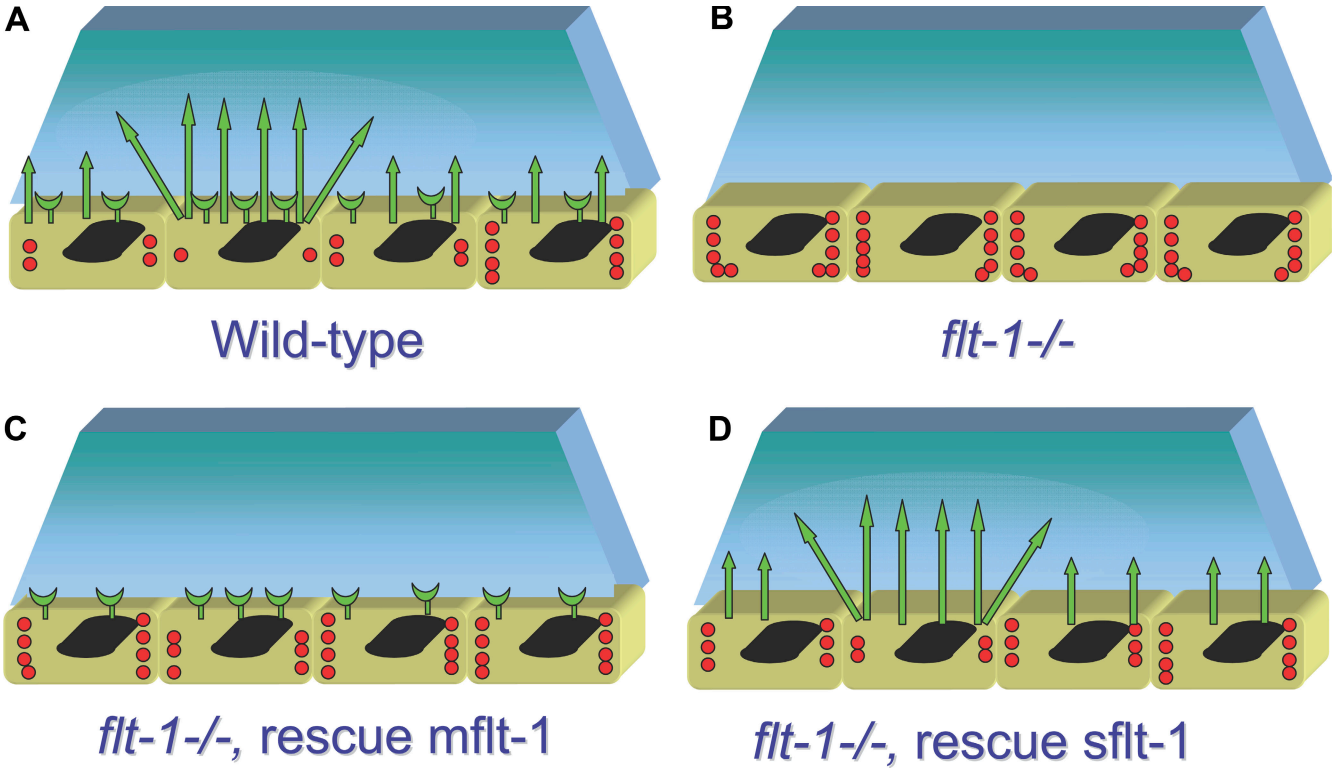

Figure 9. **Model proposing a mechanism for differential Flt-1 isoform activity in Flk signaling and branching morphogenesis.** We propose a model in which Flt-1 secreted from endothelial cells modulates a VEGF-A gradient (greenish blue) to affect ligand availability based on the heterogenous expression of both Flt-1 isoforms in developing vessels. (A) In WT vessels, both mFlt-1 and sFlt-1 act as ligand sinks to modulate the amplitude of the VEGF signal to endothelial cells. The ability of sFlt-1 to be secreted leads to the modulation of pFlk signaling in neighboring cells as well. (B) In the absence of Flt-1, the VEGF-A gradient is not modulated either quantitatively or qualitatively, which leads to excess and more uniform pFlk signaling and aberrant proliferation and branching. (C) Expression of an mFlt-1 transgene reduces overall levels of pFlk signaling, but the pattern of pFlk activation remains more homogeneous because the mFlt-1 effects are cell autonomous and do not extend to neighboring cells. Thus, proliferation but not branching is rescued. (D) Expression of an sFlt-1 transgene also reduces overall levels of Flk-1 activation and modulates signal amplitude to rescue proliferation, but the ability of sFlt-1 to be secreted allows it to modulate ligand availability to nearby cells and thus restores more of the heterogeneity of pFlk staining and rescue branching. Green arrows denote sFlt-1 protein, green cups denote mFlt-1 protein, and red dots denote pFlk expression.

mosaic pattern of Flk-1 activation in sFlt-rescued *flt-1*$^{-/-}$ mutant vessels indicates that only sFlt-1 critically regulates VEGF-A signaling that leads to proper vessel morphogenesis. We suggest that both sFlt-1 and mFlt-1 are expressed heterogeneously in developing vessels but that the impact of heterogeneous sFlt-1 expression is amplified by its ability to leave the cell surface and affect VEGF availability to nearby cells (Fig. 9, A and D). In contrast, the ability of mFlt-1 to induce heterogeneous Flk signaling is predicted to be cell autonomous and, thus, local and modest in comparison to the effects of sFlt-1 (Fig. 9 C).

Although it is not completely clear how the discontinuities of Flk-1 signaling that are formed as a result of sFlt-1 expression are achieved, it is interesting that a similar pattern of mosaic activation has recently been reported for the Notch signaling pathway in developing vessels (Hellstrom et al., 2007; Hofmann and Luisa Iruela-Arispe, 2007). Expression of the Notch ligands Dll-4 (Deltalike 4) and Jagged were found in a mosaic pattern. The VEGF-A pathway appears to function both upstream and downstream of the Notch pathway in endothelial cells because VEGF signaling was required for Dll4 expression in tumors, and VEGF receptor expression was modulated in retinas heterozygous for Dll4 (Noguera-Troise et al., 2006; Suchting et al., 2007). Interestingly, in the latter study, Flt-1 (VEGFR-1) RNA was down-regulated with the loss of Notch-Delta signaling in *Dll4*$^{+/-}$ retinas, suggesting that under normal conditions, Notch-Delta signaling up-regulates Flt-1, and this regulation may contribute to the negative regulation of tip cell formation and sprouting mediated by Notch-Delta. In this scenario, it is provocative to speculate that perhaps the spatial organization of Notch signaling influences spatial VEGF signaling or vice versa.

Recently, the importance of the Flt-1 receptor in hematopoietic stem and progenitor cell function has been established. Both homing of hematopoietic progenitors and their ability to set up a niche for metastatic tumor cells in distant organs require Flt-1, and these functions are likely mediated via the signaling properties of the Flt-1 receptor (Hattori et al., 2002; Kaplan et al., 2005). However, it has been difficult to establish a physiological role for the soluble form of the Flt-1 receptor. It is implicated in the pathology of preeclampsia in pregnant women because sFlt-1 serum levels are elevated in women with the condition, but its exact role in this placental disease is not well understood (for review see Maynard et al., 2005). A recent study in the eye showed that avascularity of the cornea, which allows for proper vision, results from the expression of soluble Flt-1 that binds VEGF-A protein (Ambati et al., 2006). Our work shows that

Published May 26, 2008

soluble Flt-1 is also critical for proper vessel morphogenesis in developing vessels and suggests that sFlt-1 exerts its effects by spatial modulation of VEGF-A signaling. Thus, it seems likely that sFlt-1 acts as an endogenous modulator of blood vessel formation in numerous physiological contexts. In some cases, its expression provides for the complete blockade of VEGF signaling, whereas in other contexts, its regulated activity modulates the presentation of VEGF-A to the developing vessel. Our increased knowledge of the antiangiogenic mechanisms used by nature to regulate blood vessel formation should aid in the development of rational therapies for vascular diseases.

Materials and methods

DNA constructs and electroporation

The PECAM promoter/intron enhancer was a gift from H. Scott Baldwin (Vanderbilt University, Nashville, TN), sFlt-1 cDNA was generated as described previously (Kearney et al., 2004), and mFlt-1 cDNA was a gift from G. Breier (University of Dresden, Dresden, Germany; Breier et al., 1995). Targeted insertion of the Flt-1 isoform transgene into the *ROSA26* genomic locus (targeting vector was a gift from P. Soriano, Fred Hutchinson Cancer Research Center, Seattle, WA) was performed using Gateway MultiSite cloning vectors. The targeting vector pROSA26-1 was modified by adding an MluI site into the lone restriction site of the multiple cloning site, XbaI. PacI was also added into the KpnI site of pROSA26-1. The resulting vector was designated modified pROSA26-1. Modified pROSA26-1 was next transformed into a Gateway destination vector. Three Gateway donor vectors were subsequently created. The first one, pDONR P2R-P3, was made as two different vectors: one containing sFlt-1 cDNA and the other containing mFlt-1 cDNA. Each PCR product (sFlt-1 and mFlt-1 transgene) was recombined into pDONR P2R-P3 via attB sites to create pDONR P2R-P3–sFlt-1 and pDONR P2R-P3–mFlt-1. The PECAM promoter/intron enhancer was then amplified, and the PCR product was recombined into pDONR-221 via attB sites to create pDONR221-PECAM. We next amplified a PGK-hygromycin cassette and recombined the PCR product into pDONR P4-P1R via attB sites to create pDONR P4-P1R-PGK-Hygro. Each Flt-1 isoform-specific pDONR-P2R-P3–Flt-1 vector was combined with pDONR221-PECAM, pDONR-P4-P1R-PGK-Hygro, and pROSA26-1 – DEST R4-R3 to create pROSA26-1-PECAM–sFlt-1–Hygro and pROSA26-1-PECAM–mFlt-1–Hygro. 15 µg of each pROSA26-1-PECAM–Flt-1–Hygro DNA was linearized with PacI and electroporated into 2×10^7 *flt-1*$^{-/-}$ ES cells using an electroporator (250 V/300 µF; GenePulser II; Bio-Rad Laboratories). Selection was in 200 µg/ml hygromycin B (Roche) for 12–14 d, and drug-resistant ES cell colonies were picked and expanded. Correct targeting into the *ROSA26* locus was confirmed via PCR using forward primer 5′-CCTAAAGAAGAGGCTGTGCTTTGG-3′ and reverse primer 5′-CCGATGGCTGTGTAGAAGTACTC-3′.

Cell culture and in vitro differentiation

WT ES cells, *flt-1*$^{-/-}$ ES cells (gift of G.-H. Fong, University of Connecticut Health Center, Farmington, CT), and *flt-1*$^{-/-}$ ES cells containing an sFlt-1 or mFlt-1 transgene linked to the PECAM promoter/intron enhancer element in the *ROSA26* locus (ROSA;Tg PECAM–sFlt-1 and ROSA;Tg PECAM–mFlt-1) were maintained and differentiated as described previously (Bautch et al., 1996; Kearney and Bautch, 2003). Embryoid bodies were plated onto either slide flasks (Thermo Fisher Scientific) or wells of a 24-well tissue culture dish at day 3 of differentiation and cultured at 37°C in 5% CO_2 until day 8, when cultures were fixed and analyzed.

Antibody staining and quantitative image analysis

Day 8 ES cell cultures were rinsed with PBS and fixed for 5 min in ice-cold methanol-acetone (50:50) for PECAM or β-galactosidase staining or 4% PFA in PBS for Flk-1 staining. For PECAM staining, fixed cultures were reacted with rat anti–mouse PECAM at 1:1,000 (MEC 13.3; BD Biosciences) and donkey anti–rat IgG (IgG; H+L) TRITC at 1:100 (Jackson ImmunoResearch Laboratories) or goat anti–rat conjugated to AlexaFluor488 (IgG; H+L) at 1:200 (Invitrogen) as described previously (Bautch et al., 2000). For β-galactosidase staining, cultures were reacted with rabbit polyclonal anti–β-galactosidase at 1:300 (Cappel Laboratories) and donkey anti–rabbit IgG (IgG; H+L) TRITC at 1:100 (Jackson ImmunoResearch Laboratories). For Flk-1 and pFlk (Tyr-1173/1175) staining, cultures were blocked in staining medium (5% goat serum in PBS) for 1 h at 37°C, and all antibodies were diluted into staining medium. Cultures were incubated in phospho–VEGFR-2 (Tyr-1175) rabbit antibody (19A10; Cell Signaling Technology) at 1:200 overnight at 4°C and after PBS washes were incubated with goat anti–rabbit IgG conjugated to AlexaFluor488 (Invitrogen) at 1:400 for 2 h at RT. Cultures were then incubated with rat anti–mouse Flk-1 antibody (BD Biosciences) at 1:200 overnight at 4°C and with goat anti–rat IgG conjugated to AlexaFluor568 (Invitrogen) for 1 h at RT and rinsed in PBS. PECAM-stained cultures were viewed and photographed with an inverted microscope (IX-50; Olympus) outfitted with epifluorescence using a 10× NA 0.25 CPlan RT objective (Olympus) and a camera (DP71; Olympus) with DP Controller version 3.1.1.267 software (Olympus). Flk-1– and β-galactosidase–stained cultures were analyzed with a confocal microscope (LSM 5 PASCAL; Carl Zeiss, Inc.) using either a 40× NA 1.3 EC Plan-Neofluor oil objective (Carl Zeiss, Inc.) or a 100× NA 1.4 plan-Apochromat oil objective (Carl Zeiss, Inc.) at RT using PASCAL Release version 4.2 SP1 acquisition software (Carl Zeiss, Inc.). For the β-galactosidase–stained cultures, ~10 confocal images were acquired through 12 µm of thickness on the z axis and were combined and flattened. Minor adjustments (brightness and contrast to the whole panel) were done using Photoshop CS2 (Adobe).

To quantify the vascular area labeled with PECAM antibody, PECAM-stained cultures were photographed and analyzed as described previously (Kearney et al., 2002). In brief, four to six wells were analyzed for each genotype. For each well, six to eight images were acquired sequentially for analysis. Percent PECAM area means for each well were calculated, and the mean of four wells for each clone was used to determine SD values. Branch point analysis was performed on similar images from PECAM-stained cultures as described previously (Kearney et al., 2004). The mean branch point score from 8–12 pictures for each clone was used to determine SD values. All values were statistically analyzed using the two-tailed *t* test. Flk-1–stained cultures were analyzed by counting the number of total Flk-1–positive cells that also were positive for pFlk (Tyr-1173/1175) in representative areas. Quantitative analysis of the ratio of pFlk (Tyr-1173/1175) to total Flk staining was performed by outlining individual endothelial cells and using MetaMorph software (MDS Analytical Technologies) to calculate the ratio.

Mitotic index analysis

ES cell cultures were differentiated to day 8 and were fixed and stained with antibodies to PECAM-1 and phosphohistone H3 as described previously (Kearney et al., 2002). Nuclei were visualized with DRAQ 5 used according to the manufacturer's protocol (Biostatus Limited). Endothelial mitotic indices were determined from confocal images as described previously (Kearney et al., 2002). Values were statistically compared using χ^2 analysis.

Real-time RT-PCR

Real-time RT-PCR was performed as described previously (Hazarika et al., 2007). In brief, total RNA was extracted from cells using the Ribopure total RNA kit (Ambion) according to manufacturer's instructions. After DNase digestion, 1 µg of total RNA was reverse transcribed using the high capacity cDNA Reverse Transcription kit (Applied Biosystems). 50 ng cDNA was amplified in a Real-Time PCR System (model 7300; Applied Biosystems) using Taqman gene expression assays specific for mFlt-1 and sFlt-1 (custom-designed Taqman assay; forward primer, 5′-GCAGAGCCAGGAACATATACACA-3′; reverse primer, 5′-GAGATCCGAGAGAAAATGGCCTTT-3′; probe, CAGTGCTCACCTCTAACG). Each sample was run in duplicate, and the expression of target was normalized to endogenous 18S ribosomal RNA. Target copies were quantified using the comparative threshold cycle relative quantitation method. Total RNA without reverse transcription was used as the nontemplate control.

Western blot analysis

Western blot analysis was performed as described previously with some modifications (Roberts et al., 2004). In brief, day 8 ES cell cultures were lysed into radioimmunoprecipitation assay buffer supplemented with protease inhibitors. Lysates were centrifuged at 12,000 *g* for 10 min, and supernatants were separated on an 8% SDS-polyacrylamide gel. Gel transfer was to a polyvinylidene fluoride membrane (GE Healthcare) under standard conditions. The phospho-Flk signal was detected by incubation with antiphospho-VEGFR2 (Tyr-1175; 1:500; Cell Signaling Technology) and HRP-labeled anti–mouse secondary antibody (1:5,000; GE Healthcare). Total Flk-1 was detected by using rat ant–mouse Flk-1 antibody (1:500; BD Biosciences) and HRP-labeled anti–rat secondary antibody (1:5,000; GE Healthcare). After detection by enhanced chemiluminescence (GE Healthcare), the results were quantified by densitometry using ImageJ (National Institutes of Health).

Published May 26, 2008

FACS analysis

Day 8 differentiated ES cell cultures were rinsed twice with PBS and dissociated with 0.5× trypsin/EDTA solution (Invitrogen) for 2–3 min. After the addition of an equal volume of FBS, cells were passed through a cell strainer (40 µm). 1×10^6 cells of each sample were rinsed once with staining medium (2% FBS in PBS) and incubated with rat anti–mouse CD102 (ICAM-2) antibody (BD Biosciences) in staining medium for 30 min on ice. After two washes with cold staining medium, cells were resuspended in staining medium with goat anti–rat IgG conjugated to FITC (Jackson ImmunoResearch Laboratories) and incubated for 30 min on ice. After two washes with cold staining medium, the cells were resuspended with 400 µl of fixation buffer (1% PFA in PBS). FACS data were collected with a CyAn ADP machine (Dako).

Online supplemental material

Fig. S1 shows FACS of day 8 ES cell cultures (WT, *flt-1* mutant, and several rescue clones) labeled with the vascular marker ICAM-2. Semiquantitative analysis of the proportion of ICAM-2–positive cells from each culture is also shown. Online supplemental material is available at http://www.jcb.org/cgi/content/full/jcb.200709114/DC1.

We thank H. Scott Baldwin, George Breier, Guo-Hua Fong, and Phil Soriano for gifts of plasmids and cells. We thank Bautch laboratory colleagues for many useful discussions, Dave Roberts for comments, and Rebecca Rapoport for technical support.

This work was supported by grants from the National Institutes of Health to V.L. Bautch (HL43174 and HL86564) and B.H. Annex (R33 HL88286) and a predoctoral fellowship from the American Heart Association to N.C. Kappas.

Submitted: 18 September 2007
Accepted: 30 April 2008

References

Ambati, B.K., M. Nozaki, N. Singh, A. Takeda, P.D. Jani, T. Suthar, R.J.C. Albuquerque, E. Richter, E. Sakurai, M.T. Newcomb, et al. 2006. Corneal avascularity is due to soluble VEGF receptor-1. *Nature.* 443:993–997.

Ashe, H.L., and J. Briscoe. 2006. The interpretation of morphogen gradients. *Development.* 133:385–394.

Autiero, M., J. Waltenberger, D. Communi, A. Kranz, L. Moons, D. Lambrechts, J. Kroll, S. Plaisance, M. De Mol, F. Bono, et al. 2003. Role of PlGF in the intra- and intermolecular cross talk between the VEGF receptors Flt1 and Flk1. *Nat. Med.* 9:936–943.

Bautch, V.L., W.L. Stanford, R. Rapoport, S. Russell, R.S. Byrum, and T.A. Futch. 1996. Blood island formation in attached cultures of murine embryonic stem cells. *Dev. Dyn.* 205:1–12.

Bautch, V.L., S.D. Redick, A. Scalia, M. Harmaty, P. Carmeliet, and R. Rapoport. 2000. Characterization of the vasculogenic block in the absence of vascular endothelial growth factor-A. *Blood.* 95:1979–1987.

Breier, G., M. Clauss, and W. Risau. 1995. Coordinate expression of vascular endothelial growth factor receptor-1 (flt-1) and its ligand suggests a paracrine regulation of murine vascular development. *Dev. Dyn.* 204:228–239.

Carmeliet, P., V. Ferreira, G. Breier, S. Pollefeyt, L. Kieckens, M. Gertsenstein, M. Fahrig, A. Vandenhoeck, K. Harpal, C. Eberhardt, et al. 1996. Abnormal blood vessel development and lethality in embryos lacking a single VEGF allele. *Nature.* 380:435–439.

Coultas, L., K. Chawengsaksophak, and J. Rossant. 2005. Endothelial cells and VEGF in vascular development. *Nature.* 438:937–945.

Ferrara, N., K. Carver-Moore, H. Chen, M. Dowd, L. Lu, K.S. O'Shea, L. Powell-Braxton, K.J. Hillan, and M.W. Moore. 1996. Heterozygous embryonic lethality induced by targeted inactivation of the VEGF gene. *Nature.* 380:439–442.

Fong, G.H., J. Rossant, M. Gertsenstein, and M.L. Breitman. 1995. Role of the Flt-1 receptor tyrosine kinase in regulating the assembly of vascular endothelium. *Nature.* 376:66–70.

Gerhardt, H., M. Golding, M. Fruttiger, C. Ruhrberg, A. Lundkvist, A. Abramsson, M. Jeltsch, C. Mitchell, K. Alitalo, D. Shima, and C. Betsholtz. 2003. VEGF guides angiogenic sprouting utilizing endothelial tip cell filopodia. *J. Cell Biol.* 161:1163–1177.

Hattori, K., B. Heissig, Y. Wu, S. Dias, R. Tejada, B. Ferris, D.J. Hicklin, Z. Zhu, P. Bohlen, L. Witte, et al. 2002. Placental growth factor reconstitutes hematopoiesis by recruiting VEGFR1+ stem cells from bone-marrow microenvironment. *Nat. Med.* 8:841–849.

Hazarika, S., A. Dokun, Y. Li, A. Popel, C. Kontos, and B. Annex. 2007. Impaired angiogenesis after hindlimb ischemia in type 2 diabetes mellitus: differential regulation of vascular endothelial growth factor receptor 1 and soluble vascular endothelial growth factor receptor 1. *Circ. Res.* 101:948–956.

Hellstrom, M., L.-K. Phng, J.J. Hofmann, E. Wallgard, L. Coultas, P. Lindbrom, J. Alva, A.-K. Nilsson, L. Karlsson, N. Gaiano, et al. 2007. Dll4 signalling through Notch 1 regulates formation of tip cells during angiogenesis. *Nature.* 445:776–780.

Hiratsuka, S., O. Minowa, J. Kuno, T. Noda, and M. Shibuya. 1998. Flt-1 lacking the tyrosine kinase domain is sufficient for normal development and angiogenesis in mice. *Proc. Natl. Acad. Sci. USA.* 95:9349–9354.

Hiratsuka, S., K. Nakao, K. Nakamura, M. Katsuki, Y. Maru, and M. Shibuya. 2005. Membrane fixation of vascular endothelial growth factor receptor 1 ligand-binding domain is important for vasculogenesis and angiogenesis in mice. *Mol. Cell. Biol.* 25:346–354.

Hofmann, J.J., and M. Luisa Iruela-Arispe. 2007. Notch expression patterns in the retina: an eye on receptor-ligand distribution during angiogenesis. *Gene Expr. Patterns.* 7:461–470.

Kaplan, R.N., R.D. Riba, S. Zacharoulis, A.H. Bramley, L. Vincent, C. Costa, D.D. MacDonald, D.K. Jin, K. Shido, S.A. Kerns, et al. 2005. VEGFR1-positive haematopoietic bone marrow progenitors initiate the pre-metastatic niche. *Nature.* 438:820–827.

Kearney, J.B., and V.L. Bautch. 2003. In vitro differentiation of mouse ES cells: hematopoietic and vascular development. *Methods Enzymol.* 365:83–98.

Kearney, J.B., C.A. Ambler, K.A. Monaco, N. Johnson, R.G. Rapoport, and V.L. Bautch. 2002. Vascular endothelial growth factor receptor Flt-1 negatively regulates developmental blood vessel formation by modulating endothelial cell division. *Blood.* 99:2397–2407.

Kearney, J.B., N.C. Kappas, C. Ellerstrom, F.W. DiPaola, and V.L. Bautch. 2004. The VEGF receptor flt-1 (VEGFR-1) is a positive modulator of vascular sprout formation and branching morphogenesis. *Blood.* 103:4527–4535.

Kendall, R.L., and K.A. Thomas. 1993. Inhibition of vascular endothelial cell growth factor activity by an endogenously encoded soluble receptor. *Proc. Natl. Acad. Sci. USA.* 90:10705–10709.

Koleske, A.J. 2003. Do filopodia enable the growth cone to find its way? *Sci. STKE.* doi:10.1126/stke.2003.183.pe20.

Kowanetz, M., and N. Ferrara. 2006. Vascular endothelial growth factor signaling pathways: therapeutic perspective. *Clin. Cancer Res.* 12:5018–5022.

Maynard, S.E., S. Venkatesha, R. Thadhani, and S. Karumanchi. 2005. Soluble fms-like tyrosine kinase 1 and endothelial dysfunction in the pathogenesis of preeclampsia. *Pediatr. Res.* 57:1R–7R.

Miquerol, L., B.L. Langille, and A. Nagy. 2000. Embryonic development is disrupted by modest increases in vascular endothelial growth factor gene expression. *Development.* 127:3941–3946.

Neagoe, P.-E., C. Lemieux, and M.G. Sirois. 2005. Vascular endothelial growth factor (VEGF)-A165-induced prostacyclin synthesis requires the activation of VEGF receptor-1 and -2 heterodimer. *J. Biol. Chem.* 280:9904–9912.

Noguera-Troise, I., C. Daly, N. Papadopoulos, S. Coetzee, P. Boland, N. Gale, H. Lin, G. Yancopoulos, and G. Thurston. 2006. Blockade of Dll4 inhibits tumour growth by promoting non-productive angiogenesis. *Nature.* 444:1032–1037.

Orecchia, A., P. Lacai, C. Schietroma, V. Morea, G. Zambruno, and C. Failla. 2003. Vascular endothelial growth receptor-1 is deposited in the extracellular matrix by endothelial cells and is a ligand for the α5β1 integrin. *J. Cell Sci.* 116:3479–3489.

Park, M., and S. Lee. 1999. The fourth immunoglobulin-like loop in the extracellular domain of FLT-1, a VEGF receptor, includes a major heparin-binding site. *Biochem. Biophys. Res. Commun.* 264:730–734.

Rahimi, N. 2006. VEGFR-1 and VEGFR-2: two non-identical twins with a unique physiognomy. *Front. Biosci.* 11:818–829.

Risau, W. 1997. Mechanisms of angiogenesis. *Nature.* 386:671–674.

Roberts, D.M., J.B. Kearney, J.H. Johnson, M.P. Rosenberg, R. Kumar, and V.L. Bautch. 2004. The vascular endothelial growth factor (VEGF) receptor Flt-1 (VEGFR-1) modulates Flk-1 (VEGFR-2) signaling during blood vessel formation. *Am. J. Pathol.* 164:1531–1535.

Ruhrberg, C., H. Gerhardt, M. Golding, R. Watson, S. Ioannidou, H. Fujisawa, C. Betsholtz, and D.T. Shima. 2002. Spatially restricted patterning cues provided by heparin-binding VEGF-A control blood vessel branching morphogenesis. *Genes Dev.* 16:2684–2698.

Sakurai, Y., K. Ohgimoto, Y. Kataoka, N. Yoshida, and M. Shibuya. 2005. Essential role of Flk-1 (VEGF receptor 2) tyrosine residue 1173 in vasculogenesis in mice. *Proc. Natl. Acad. Sci. USA.* 102:1076–1081.

Shibuya, M. 2006. Vascular endothelial growth factor receptor 1 (VEGFR-1/Flt-1): a dual regulator for angiogenesis. *Angiogenesis.* 9:225–230.

Published May 26, 2008

Shibuya, M., and L. Claesson-Welsh. 2006. Signal transduction by VEGF receptors in regulation of angiogenesis and lymphangiogenesis. *Exp. Cell Res.* 312:549–560.

Soriano, P. 1999. Generalized lacZ expression with the ROSA26 Cre reporter strain. *Nat. Genet.* 21:70–71.

Srinivas, S., T. Watanabe, C. Lin, C. William, Y. Tanabe, T. Jessell, and F. Costantini. 2001. Cre reporter strains produced by targeted insertion of EYFP and ECFP into the ROSA26 locus. *BMC Dev. Biol.* 1:4.

Stalmans, I., Y.S. Ng, R. Rohan, M. Fruttiger, A. Bouche, A. Yuce, H. Fujisawa, B. Hermans, M. Shani, S. Jansen, et al. 2002. Arteriolar and venular patterning in retinas of mice selectively expressing VEGF isoforms. *J. Clin. Invest.* 109:327–336.

Suchting, S., C. Freitas, F. le Noble, R. Benedito, C. Breant, A. Duarte, and A. Eichmann. 2007. The Notch ligand Delta-like 4 negatively regulates endothelial tip cell formation and vessel branching. *Proc. Natl. Acad. Sci. USA.* 104:3225–3230.

Tischer, E., R. Mitchell, T. Hartman, M. Silva, D. Gospodarowicz, J. Fiddes, and J. Abraham. 1991. The human gene for vascular endothelial growth factor. Multiple protein forms are encoded through alternative exon splicing. *J. Biol. Chem.* 266:11947–11954.